processes

MDPI

Article

Structure and Selected Properties of Si(C,N) Coatings on Ni-Cr Prosthetic Alloys

Zofia Kula [1], Katarzyna Dąbrowska [2] and Leszek Klimek [3,*]

[1] Department of Dental Technology, Medical University of Lodz, 251 Pomorska Street, 92-213 Lodz, Poland; zofia.kula@umed.lodz.pl
[2] Department of Endodontics, Chair of Conservative Dentistry and Endodontics, Medical University of Lodz, 251 Pomorska Street, 92-213 Lodz, Poland; katarzyna.anna.dabrowska@umed.lodz.pl
[3] Institute of Materials Science and Engineering, Faculty of Mechanical Engineering, Lodz University of Technology, ul. B. Stefanowskiego 1/15, 90-924 Lodz, Poland
* Correspondence: leszek.klimek@p.lodz.pl

Abstract: Metal alloys continue to be, and are expected to remain, essential materials for fabricating prosthetic elements due to their unique properties, particularly their high strength, durability, and appropriate modulus of elasticity, which make them well-suited for such applications. However, commonly used non-precious metal alloys exhibit lower corrosion resistance compared to precious metal alloys. This reduced resistance leads to the release of metal ions from the alloy into the oral environment. Adverse biological responses to metal alloys can be mitigated through various surface modifications, most commonly by applying coatings. These coatings are typically ceramic, including oxides, nitrides, and carbides. In this study, the mechanical properties (hardness, modulus of elasticity, adhesion, and thickness) of complex Si(C,N) coatings applied to a prosthetic Ni-Cr alloy were investigated. Depending on the proportions of N, C, and Si in the coating, the hardness ranged from 12 to 15 GPa, while the modulus of elasticity varied between 130 and 170 GPa. Adhesion strength, measured via the scratch test method, was within an acceptable range. Microscopic analysis revealed that the coatings had a thickness of 2 to 2.5 µm, exhibiting a homogeneous, columnar structure. In conclusion, the properties of the fabricated Si(C,N) coatings are deemed satisfactory for their intended use as protective layers for prosthetic and orthodontic components.

Keywords: adhesion; dental alloys; Si(C,N) coatings; mechanical properties

check for updates

Academic Editors: Sake Wang, Nguyen Tuan Hung and Minglei Sun

Received: 31 January 2025
Revised: 18 February 2025
Accepted: 20 February 2025
Published: 22 February 2025

Citation: Kula, Z.; Dąbrowska, K.; Klimek, L. Structure and Selected Properties of Si(C,N) Coatings on Ni-Cr Prosthetic Alloys. *Processes* **2025**, *13*, 624. https://doi.org/10.3390/pr13030624

Copyright: © 2025 by the authors. Licensee MDPI, Basel, Switzerland. This article is an open access article distributed under the terms and conditions of the Creative Commons Attribution (CC BY) license (https://creativecommons.org/licenses/by/4.0/).

1. Introduction

Despite progress in materials engineering, no alternative materials currently possess comparable properties. Metal alloys used in prosthetic restorations and orthodontic components within the oral cavity are commonly categorized into precious alloys (primarily gold alloys with platinum, silver, and palladium) and non-precious alloys (including titanium and its alloys, as well as cobalt–chromium and nickel–chromium alloys). For economic and technological reasons, non-precious alloys such as cobalt–chromium (Co-Cr) and nickel–chromium (Ni-Cr) are more commonly utilized in dental prosthetics. However, these alloys exhibit relatively lower corrosion resistance compared to precious metal alloys [1–5]. Their use is largely driven by economic considerations. A potential drawback of using non-precious alloys is the risk of adverse biological responses, such as allergic reactions. These reactions can be triggered by corrosion products and metal ions released during the corrosion process, which may infiltrate surrounding tissues. To mitigate these risks,

surface layer modifications are often employed to enhance biocompatibility and improve the durability of alloy components. These modifications typically involve the application of various types of coatings, achieved through techniques such as physical vapor deposition (PVD), chemical vapor deposition (CVD), and sol–gel processes [6–12]. The coatings are predominantly composed of oxides, nitrides, and carbides, which are classified as ceramics and characterized by their high chemical resistance. This property significantly reduces the corrosion of coated elements [13–15]. Beyond minimizing corrosion, these coatings act as diffusion barriers, effectively limiting the release and penetration of metal ions from the alloys into the surrounding environment [16]. These modifications contribute to reducing or even eliminating adverse biological responses. During mastication, prosthetic materials may experience abrasive wear and fretting wear. The application of coatings offers the additional benefit of enhancing the durability of prosthetic and orthodontic components within the oral cavity [17,18]. Furthermore, many coatings exhibit properties that limit the adhesion of bacteria and fungi, thereby inhibiting biofilm formation and facilitating the maintenance of proper hygiene for prosthetic restorations [7,19–22].

For coatings to effectively serve their intended purpose, they must exhibit a range of essential properties. Adequate corrosion protection primarily depends on the coatings' integrity, which requires them to be free of defects such as cracks and porosity. Furthermore, appropriate mechanical properties are critical. Prosthetic elements come into contact with teeth, where enamel hardness can reach approximately 450 HV. Coatings that are too soft may wear down prematurely, exposing the underlying alloy and compromising its protective function. Additionally, during the use of prosthetic elements, various forces act upon them, leading to deformation. The coating must possess sufficient flexibility to deform alongside the underlying alloy. To prevent the coating from delaminating or cracking, it must possess an appropriate modulus of elasticity, ideally closely matching that of the coated material. A significant disparity between the moduli can lead to the destruction of the coating. However, the most critical parameter characterizing coatings is their adhesion to the alloy. During the use of prosthetic and orthodontic elements, the coating must remain firmly attached; otherwise, delamination will compromise the protective properties.

In recent years, carbon and silicon nitrides (SiCN) have gained significant popularity due to their excellent mechanical, tribological, and optical properties, as well as their high hardness [18,23–29]. Silicon–carbon nitride (SiCN), produced by incorporating nitrogen into SiC, also exhibits strong antibacterial properties [18,27,30]. Silicon carbide (SiC) is an interesting coating material with a number of unique properties such as a high melting point, high strength, chemical stability, and electrical conductivity ideal for semiconductor applications. It has a relatively high thermal conductivity, which is not a typical characteristic of ceramic materials, and, in terms of mechanical properties, high hardness, stiffness, and high wear resistance [31]. The combination of these properties indicates its potential applicability as a material for friction pairs. The wear factor is an important parameter that describes the tribological properties of materials used in the production of prosthetic restorations [31,32]. The current literature indicates that abrasive wear is one of the causes of damage to prosthetic elements [31–33]. The wear mechanism contributes to the shortened lifespan of prosthetic elements, implants, and bridges [32,33]. The application of coatings solves wear problems [34]. Furthermore, these coatings are biocompatible and demonstrate no harmful effects when in contact with living tissues. The properties of SiCN coatings can be tailored by adjusting the ratios of silicon, carbon, and nitrogen in their composition. SiCN layers can be fabricated by combining binary materials such as SiN1.3, SiC, and CN, using techniques like chemical vapor deposition (CVD), plasma-enhanced CVD (PECVD), ion beam sputtering, and pulsed laser deposition [23]. In our previous studies, the reactive magnetron sputtering (RMS) method was employed to obtain uniform,

smooth Si(C,N)-type coatings [35]. The application of these coatings helps reduce surface roughness, which can facilitate the cleanliness of prosthetic elements. The most commonly used method for applying these coatings is plasma-enhanced chemical vapor deposition (PECVD). Xia, X. et al. [26] and Chiang [36] successfully obtained SiCN layers through PECVD by regulating the gas flow rates of ammonia (NH_3), methane (CH_4), and silane (SiH_4). Petersson et al. [37] developed SiCN coatings for use on artificial joints. Surface modification of titanium alloys for medical implants is a well-established practice [38]. However, there are no reports in the literature regarding the use of Si(C,N) coatings to modify the properties of alloys used in dental prosthetics, particularly as barrier coatings to prevent the transfer of substrate ions into the oral cavity. The favorable mechanical and antibacterial properties of these coatings could also enhance the functional performance of prosthetic and orthodontic components.

The aim of this study was to investigate the selected properties of Si(C,N) coatings on prosthetic alloys, with a focus on how carbon and nitrogen content influences these properties. The parameters chosen for investigation included coating thickness, modulus of elasticity, hardness, adhesion, and the distribution of coating elements within the coating's depth.

2. Materials and Methods

The research material consisted of cylindrical specimens with a diameter of 8 mm and a height of 10 mm, made from Ni-Cr alloy (Figure 1).

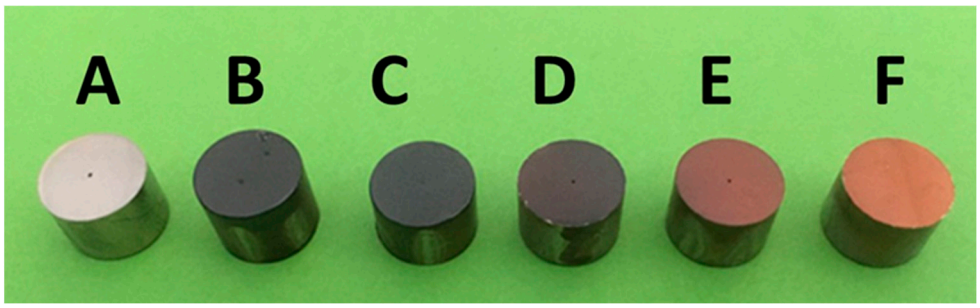


Figure 1. Tested specimens.

A total of 25 specimens were divided into five groups, each coated with Si(C,N) layers containing varying carbon and nitrogen concentrations. Prior to coating application, the surfaces of the cylinders were polished, achieving a Ra parameter value ranging from 0.378 to 0.424. The surface of the samples was ground on abrasive paper with a grit of up to 1200 and then polished using Al_2O_3 suspension. Before the coating application process, they were cleaned in a mixture of water and detergent and then cleaned in acetone using an ultrasonic cleaner. Then, they were subjected to ion cleaning. Correct preparation of the metal surface is very important because it influences the adhesion of the coating. A contaminated surface can reduce the adhesion of the coating.

The chemical composition of the alloy, the coating application conditions, and their composition have been described in earlier works [35].

The coatings were deposited with magnetron sputtering. The diagram of this method is shown in Figure 2.

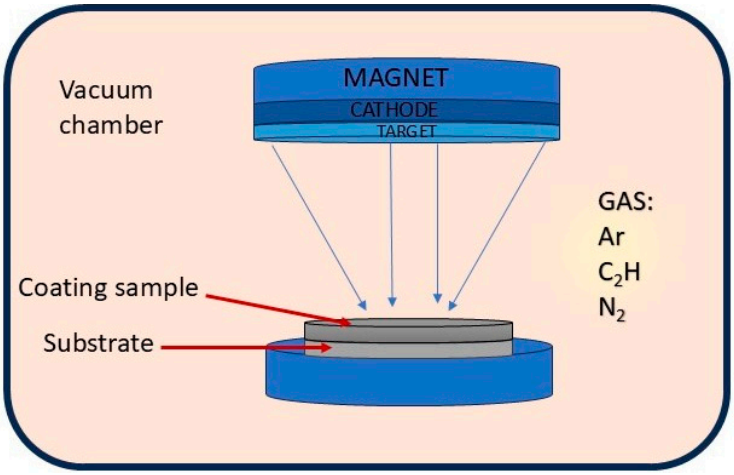


Figure 2. Schematic of the Si (C,N) coating method with PVD magnetron sputtering.

Table 1 lists the equipment used to apply the coatings.

Table 1. Equipment used for the experiment.

Equipment	Company
Planar magnetrons WK100	Dora POWER SYSTEMS, Wrocław, Poland
Vacuum chamber of the B-90 deposition apparatus	Hoch-Vacuum, Dresden, Germany

Table 2 shows the detailed parameters of the Si (C, N) coating deposition process.

Table 2. Reactive gas flow.

Gas	Flow Unit	Sample					Time [min]
		B	C	D	E	F	
N2	SCCM	28	21	14	7	-	240
C_2H_2		-	5	10	14	19	

The designations for each specimen group, along with the content of individual elements in the coatings, are presented in Table 3.

Table 3. Designation of specimen groups and contents of individual elements in the coatings.

Specimen	Element						at. C/N
	Si		N		C		
	at. [%]	wt. [%]	at. [%]	wt. [%]	at. [%]	wt. [%]	
B	24.8	38.5	-	-	75.2	61.5	-
C	29.6	46.7	15.9	12.5	54.5	40.8	3.4
D	35.2	53.3	25.2	19.0	39.6	27.7	1.6
E	42.9	61.0	35.3	25.0	21.8	14.0	0.6
F	47.7	64.7	52.3	35.3	-	-	-

Specimens with different coatings were subjected to testing to determine the hardness, modulus of elasticity, and adhesion of the coating to the alloy.

The measurements of the modulus of elasticity and hardness of the coatings were conducted using the nanoindentation method with a Nano Indenter G200 device (MTS, Eden

Prairie, MN, USA), utilizing the Continuous Load Segment (CLS) mode. The procedure involves continuously pressing an indenter (Bekovich-type in this case) into the material, followed by unloading. This results in two curves being obtained: a loading curve and an unloading curve. The loading curve is used to determine the hardness, while the unloading curve is employed to calculate the modulus of elasticity of the tested material [39,40]. The indenter was pressed to a depth of approximately 2 µm, which was sufficient for determining the modulus and hardness values of the coatings. The obtained loading and unloading curves are presented in Figure 2 and Figure 3, while Figures 4 and 5 display the hardness and modulus values for the individual coatings.

Coating adhesion to the substrate was assessed using the scratch test method with the UMT2 device (Bruker, Billerica, MA, USA). The tests were conducted by gradually increasing the load force from 0 to 10 N, with the following operating parameters: loading speed of 100 N/min, indenter speed of 10 mm/min, scratch length of approximately 9.5 mm, and the use of a Rockwell indenter.

Coating thickness measurements were performed by observing specimen fractures using an S3000N scanning electron microscope (Hitachi, Tokyo, Japan). The substrates, which were thin (0.1 mm) sheets of Ni-Cr alloy, were fractured in liquid nitrogen. Observations and measurements were conducted in BSE (backscattered electron) imaging mode with a magnification of 10,000×. This imaging technique was chosen to enhance the visibility of the coating, allowing for measurements with so-called "atomic contrast". For each coating, five measurements were made at different fracture locations. The distribution of elements within the coating depth was analyzed using a GDS 850A glow discharge optical emission spectrometer (Leco, St. Joseph, MI, USA), equipped with an RF (radio frequency) alternating current lamp and a 4 mm anode. This device enables continuous quantitative analysis of the surface layer profile

3. Results

Figures 3 and 4 present graphs obtained from the nanoindentation test. The graph in Figure 3 illustrates the variation in the hardness of individual coatings as a function of the depth of the penetrator indentation. Similarly, the graph in Figure 4 depicts the change in the modulus of elasticity with depth.

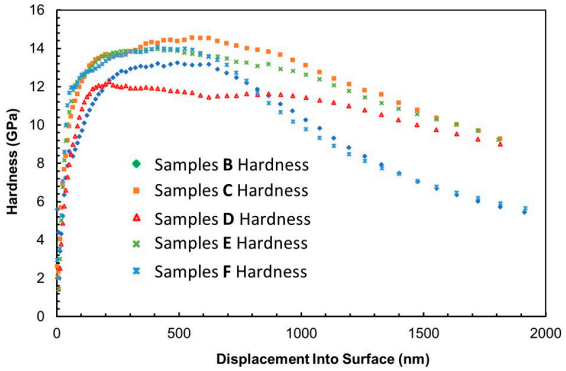


Figure 3. Hardness as a function of depth of the forced-in penetrator.

As observed from the presented graphs, both the hardness and modulus of elasticity initially stabilize but then undergo changes. This behavior is attributed to the fact that, during the penetration of the indenter into the coating, the metal substructure's influence becomes apparent at a certain depth. As a result, at greater depths, the measured parameters reflect a combination of the values for both the substructure and the coating. Consequently, the hardness and modulus of elasticity values presented in Figures 5 and 6 were calculated

for the regions of the individual coatings, specifically for values within a depth range of up to 500 nm.

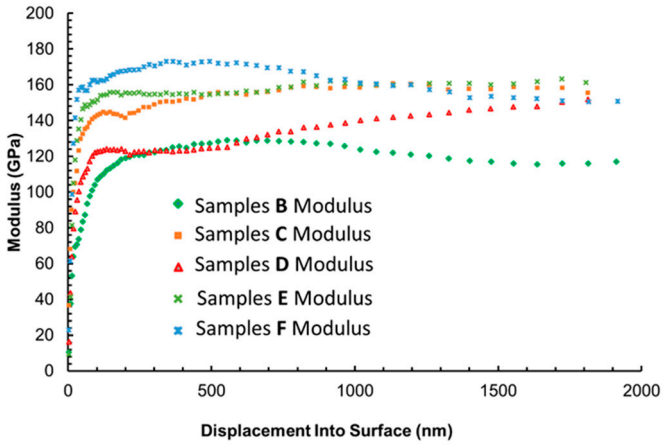


Figure 4. Moduli of elasticity as a function of depth of the forced-in penetrator.

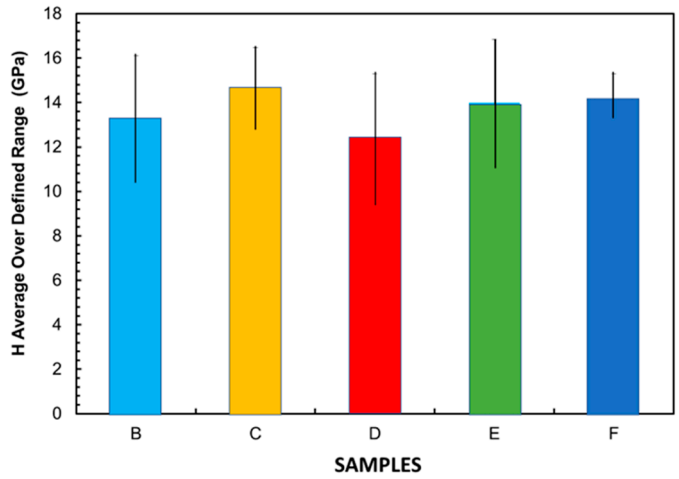


Figure 5. Hardness of tested coatings.

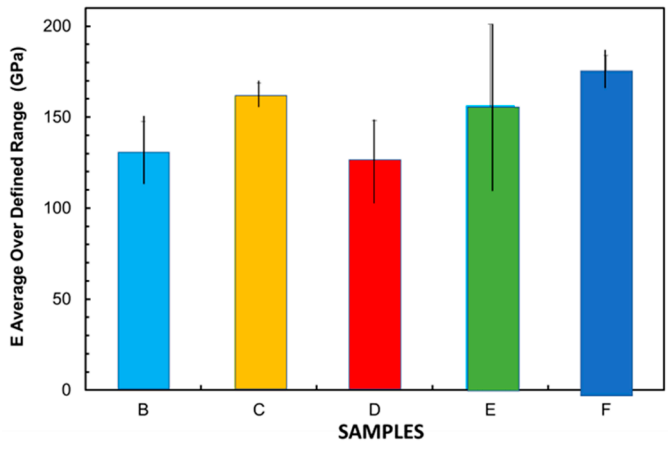


Figure 6. Modulus of elasticity of the tested coatings.

The hardness values of the tested coatings were found to range between 12 and 15 GPa.

The elastic moduli of the tested coatings were determined to be within the range of 130 to 170 GPa.

Figures 7–11 illustrate the tangential force, coefficient of friction, and acoustic emission signals as functions of the normal force and penetrator distance for the tested specimens.

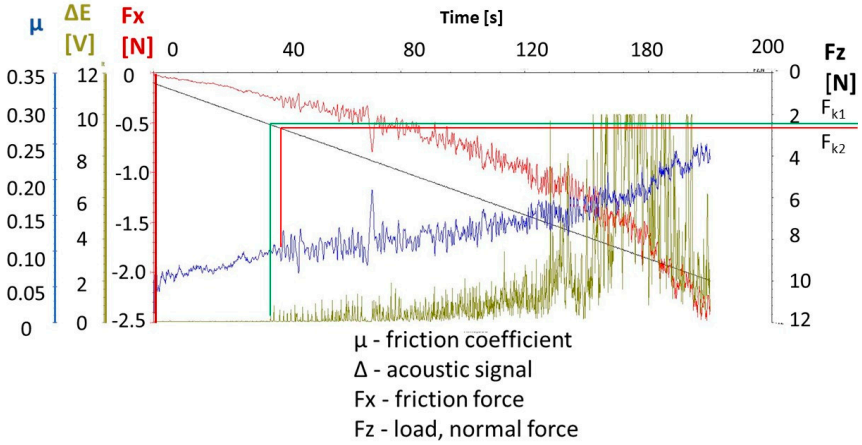


Figure 7. The coefficient of friction and acoustic emission signals with a normal force and penetrator distance for the B specimen.

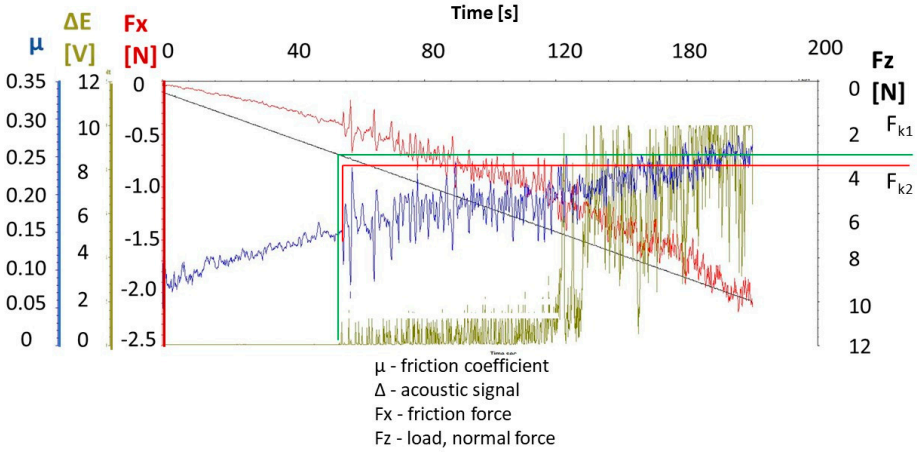


Figure 8. The coefficient of friction and acoustic emission signals with a normal force and penetrator distance for the C specimen.

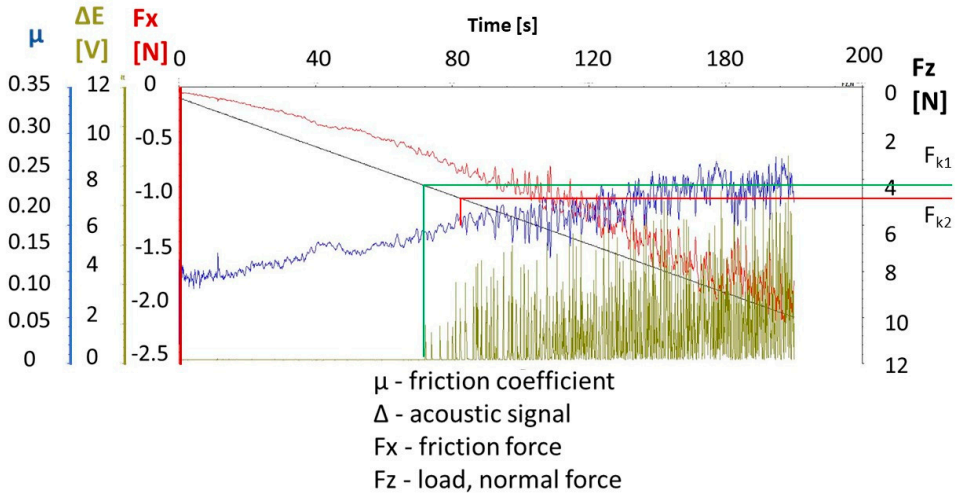


Figure 9. The coefficient of friction and acoustic emission signals with a normal force and penetrator distance for the D specimen.

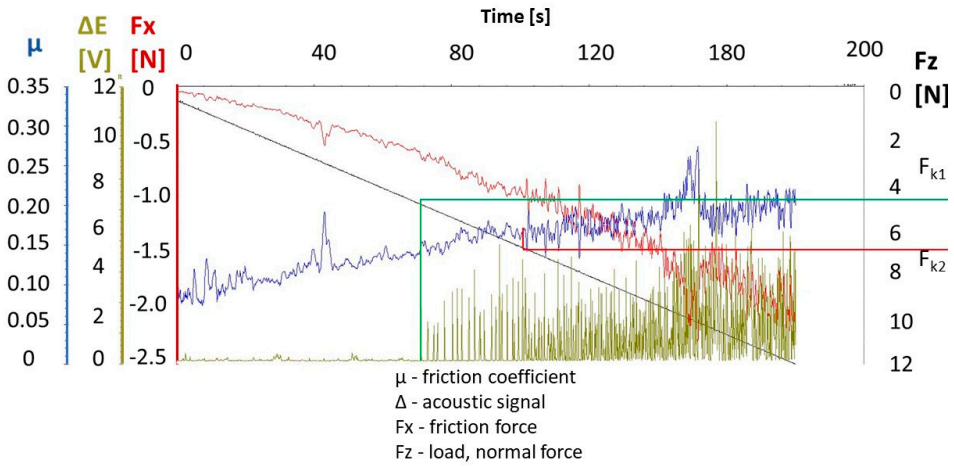


Figure 10. The coefficient of friction and acoustic emission signals with a normal force and penetrator distance for the E specimen.

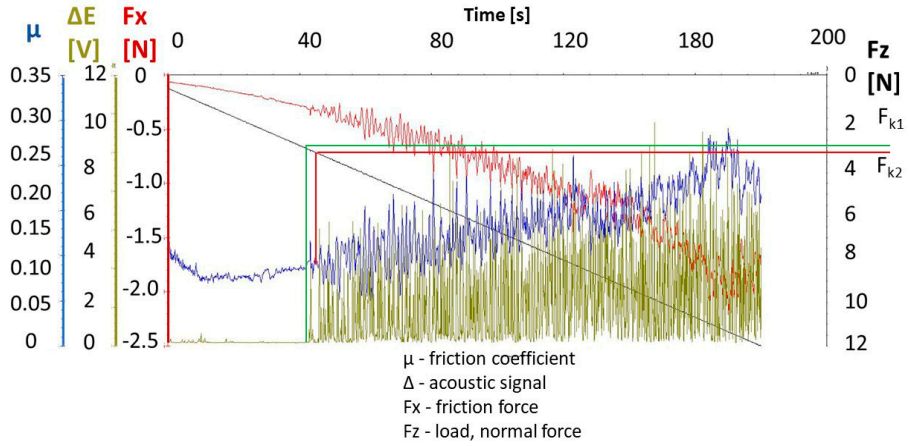


Figure 11. The coefficient of friction and acoustic emission signals with a normal force and penetrator distance for the F specimen.

The graphs for all specimens revealed sudden spikes in the acoustic emission signal, corresponding to the initiation of cracks in the coating. The subsequent increase in the friction coefficient is indicative of coating delamination. Notably, the acoustic emission signal does not directly align with changes in the friction coefficient. The graphs also display the penetrator load force (F_{zN}) at which the coating begins to crack; this force is denoted as F_{k1} in Table 4 Additionally, changes in the coefficient of friction between the penetrator and the coating surface can be observed, reflected in a more jagged and irregular graph. This indicates the onset of friction with the exposed metal substructure. At this point, the critical force for substrate exposure can be identified and is denoted as F_{k2} in Table 4. The values of the critical forces, determined from the graphs, are summarized in table.

Table 4. Critical breaking forces of the tested coatings.

Specimen	B	C	D	E	F
F_{k1}	~2.5 N	~3.5 N	~4.0 N	~4.5 N	~3 N
F_{k2}	~2.6 N	~3.7 N	~4.5 N	~7.0 N	~3.5 N

Figures 12–16 depict the scratch images obtained after performing the adhesion test.

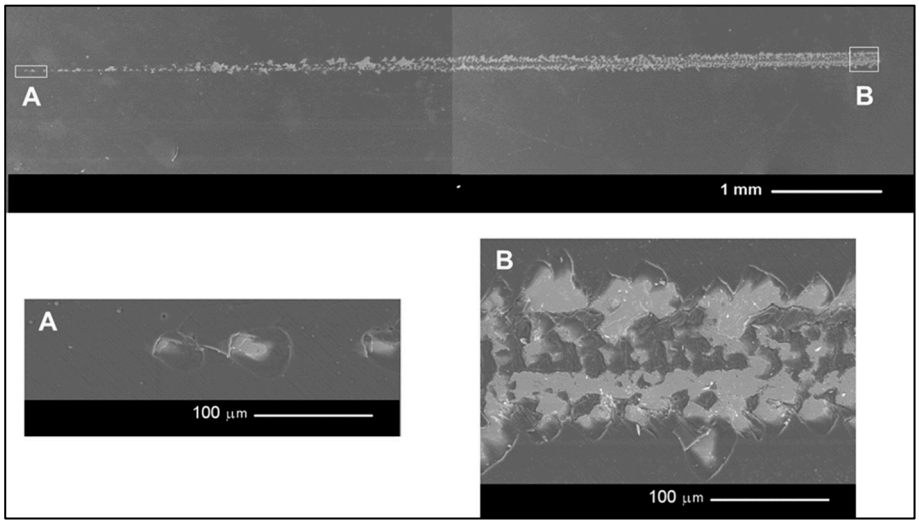


Figure 12. The image of the scratch after the scratch test on sample B, with enlarged areas at the beginning (**A**) and end (**B**) of the scratch.

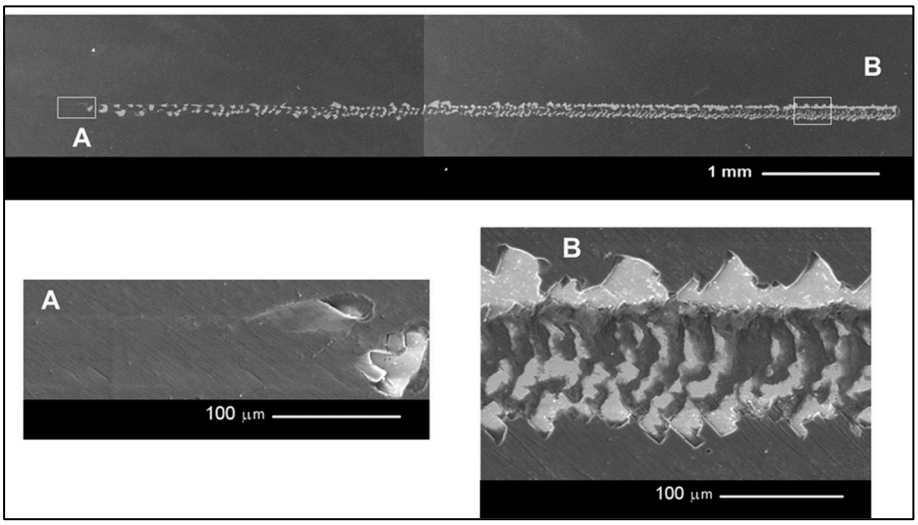


Figure 13. The image of the scratch after the scratch test on sample C, with enlarged areas at the beginning (**A**) and end (**B**) of the scratch.

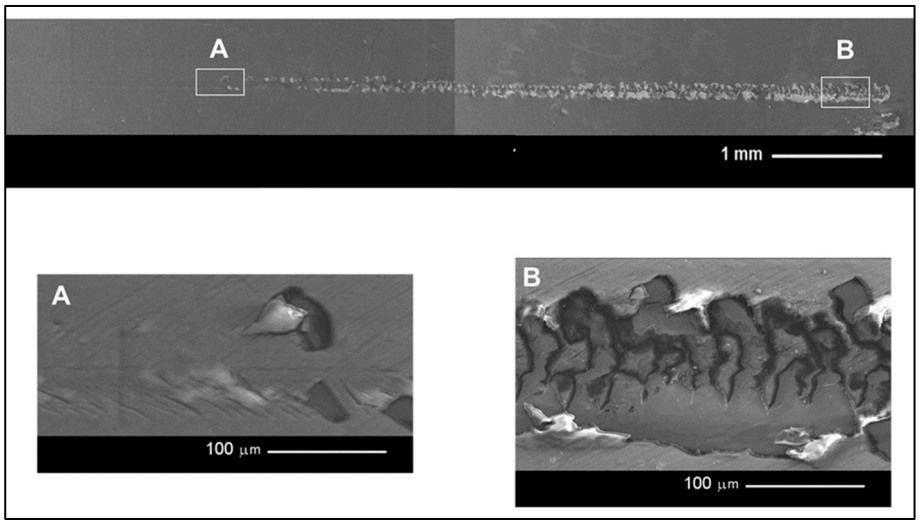


Figure 14. The image of the scratch after the scratch test on sample D, with enlarged areas at the beginning (**A**) and end (**B**) of the scratch.

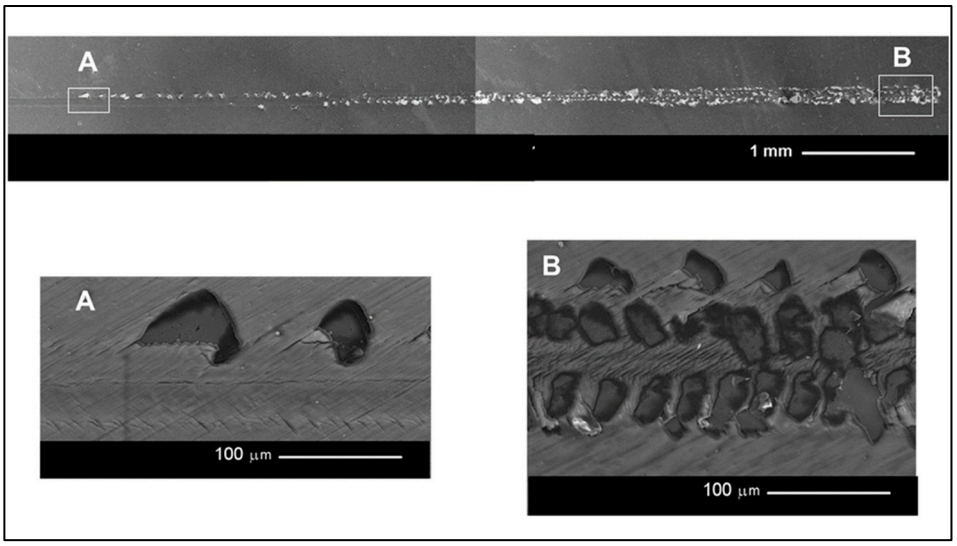


Figure 15. The image of the scratch after the scratch test on sample E, with enlarged areas at the beginning (**A**) and end (**B**) of the scratch.

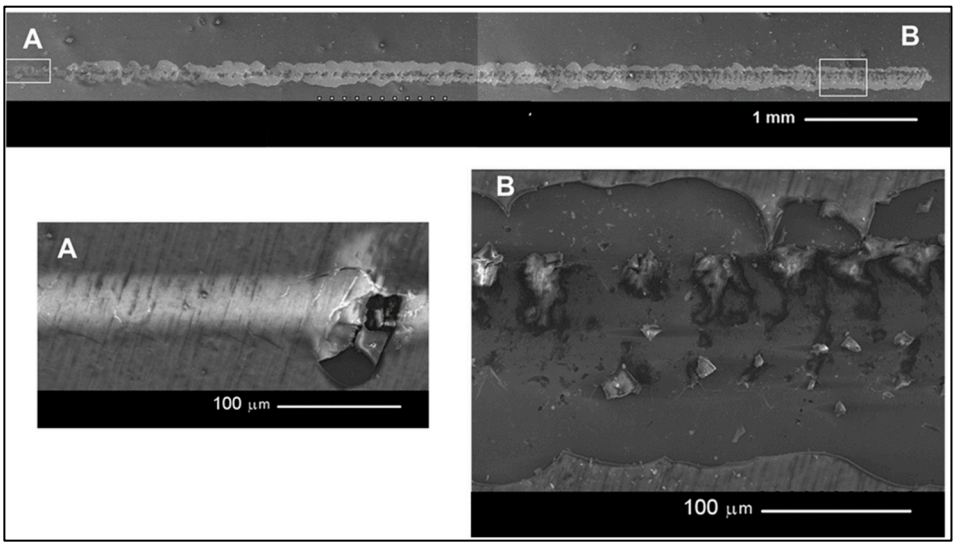


Figure 16. The image of the scratch after the scratch test on sample F, with enlarged areas at the beginning (**A**) and end (**B**) of the scratch.

The presented microscopic images distinctly reveal a two-stage coating failure mechanism. In the initial phase, cracking occurs, characterized by small cracks that grow in size as the load increases. In the subsequent phase, delamination of the coating from the substructure becomes evident, starting locally and progressively extending over larger areas until the metal substrate is fully exposed and scratched. These regions of coating damage correspond closely with the critical points observed in the scratch test graphs.

Figures 17–21 present examples of fracture images of the coated specimens, which were used to calculate the average thicknesses of the individual coatings.

The measured thickness values are summarized in Table 5.

As observed in the microscopic images of the specimens, the coatings achieved a thickness ranging from approximately 2 to 2.5 µm. The small standard deviations suggest that there is minimal variation in coating thickness across different areas of the cross-sections. The coatings appear uniform, with no visible defects or discontinuities. Furthermore, the images reveal the columnar structure of the deposited coatings

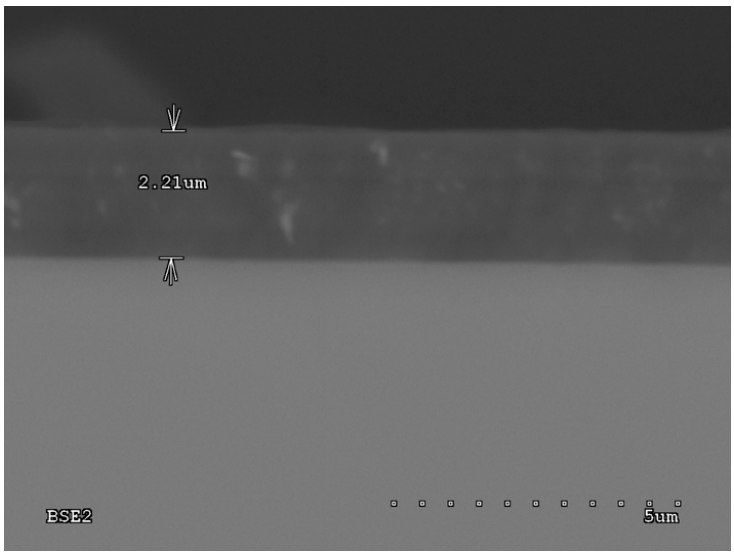


Figure 17. SEM BSE image of the fracture of specimen B.

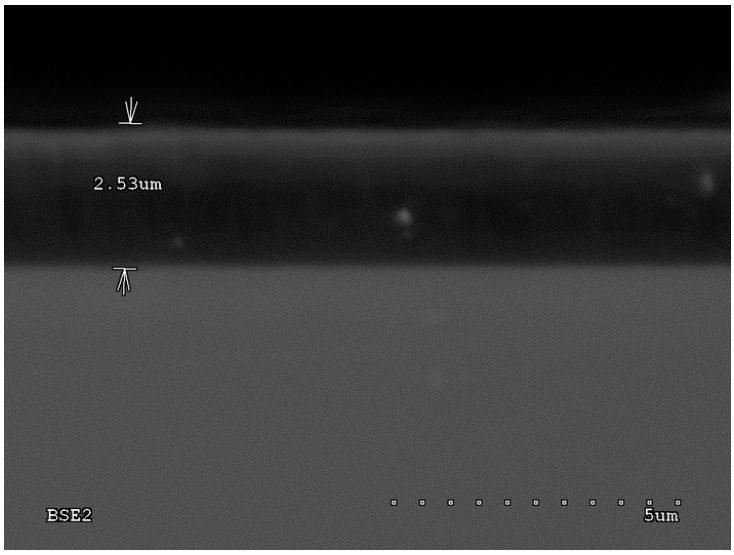


Figure 18. SEM BSE image of the fracture of specimen C.

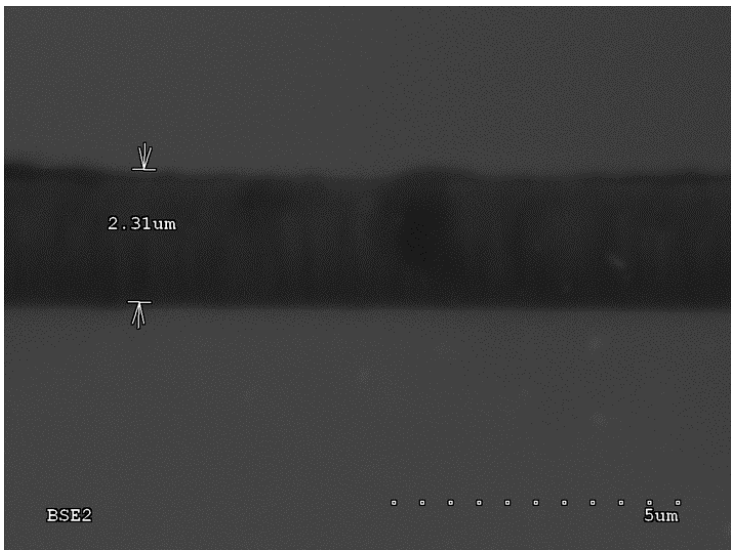


Figure 19. SEM BSE image of the fracture of specimen D.

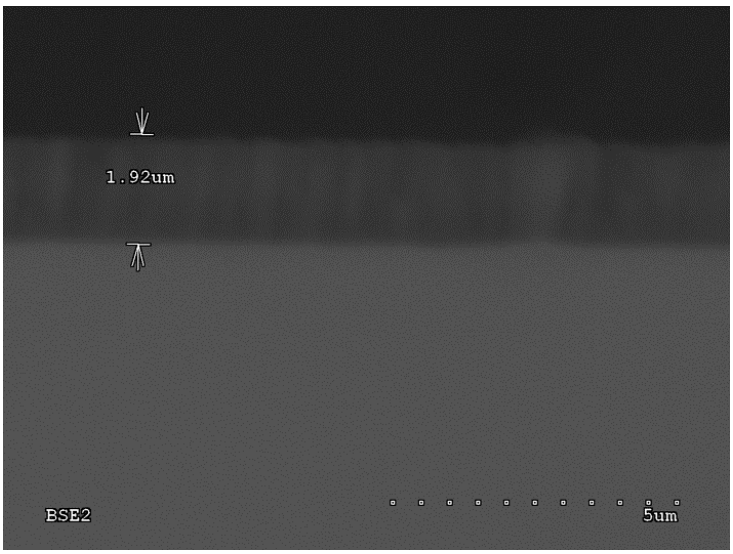


Figure 20. SEM BSE image of the fracture of specimen E.

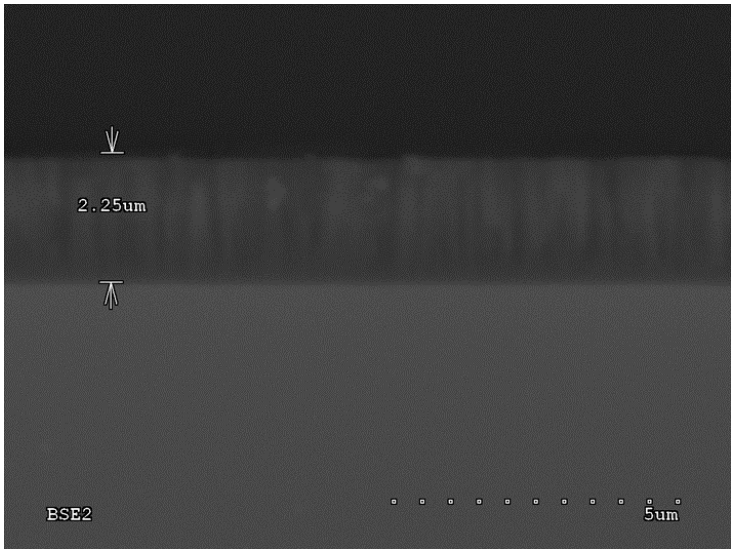


Figure 21. SEM BSE image of the fracture of specimen F.

Table 5. Average thickness values of the coatings.

	Group				
	B	**C**	**D**	**E**	**F**
Average value	2.24	2.59	2.32	1.95	2.23
SD	0.09	0.09	0.05	0.04	0.03

4. Discussion

There are no existing reports on the use of Si(C,N) coatings on Ni-Cr-type alloys. However, a few studies, such as the study by Xia et al., have utilized Si(C,N) coatings for dental implants, employing the PECVD technique [26]. Therefore, comparisons in this work will be made either with other coatings on Ni-Cr alloys or SiC and SiN coatings on different substrates. Upon analyzing the results for hardness and modulus of elasticity, no significant correlation was found between the nitrogen and carbon content in the Si(C,N) coatings. Given the high values of the standard deviation, it is apparent, even without statistical analysis, that the coatings exhibit similar hardness and modulus of

elasticity values. The absence of a dependence on chemical composition can be attributed to the amorphous nature of these coatings [35]. In contrast, crystalline coatings exhibit properties that are influenced by stoichiometry, and the introduction of additional atoms can introduce defects and stresses within the crystal lattice, which in turn affects the mechanical properties. However, in amorphous coatings, the incorporation of dopants does not significantly impact the structural defects, and thus the properties remain relatively unchanged. The measured modulus of elasticity, which is in the range of 150 GPa, is lower than that of the substrate alloy (approximately 200 GPa). Despite this, the values are deemed satisfactory, as the coatings are expected to maintain their integrity without cracking or delaminating during the deformation of the prosthetic element during use. Considering the hardness of the coatings, which ranges from 12 to 17 GPa, it is deemed sufficient. This hardness is higher than that of the substrate alloy, thus contributing to the protection of the underlying material against abrasion. During use, the surface should resist abrasive wear, preventing exposure of the substrate and maintaining the protective properties of the coating. However, it is important to note that hardness alone serves as an approximate indicator of wear resistance. Further research should focus on evaluating the tribological wear of the coatings, including wear due to friction, and fretting wear, both in dry conditions and within artificial environments.

The authors Pettersson et al. [36] investigated the deposition of silicon nitride (SiN) and silicon-carbon nitride (SiCN) coatings using the high-power pulsed magnetron sputtering (HiPIMS) method. They achieved coating hardness in the range of 10–18 GPa and elastic moduli ranging from 150 to 200 GPa. These values are slightly higher than those obtained in the current study. The difference may be attributed to variations in coating compositions and structures. Notably, the coatings in their study were applied to joint implants made of cobalt–chromium alloys. Further studies on implant coatings made from Co-Cr alloys were conducted by Skjöldebrand et al. [29], who utilized the combinatorial deposition method to obtain Si-Fe-C-N coatings. Their hardness measurements revealed values ranging from 13.7 to 17.3 GPa, while the modulus of elasticity was found to be in the range of 190–212 GPa. The differences observed between their results and those obtained in this study are likely due to the chemical composition, as no iron was present in our coatings. Additionally, it is important to note that their study employed a different deposition technique, which may have also influenced the resulting properties. The existing literature on the use of such coatings in dentistry remains limited.

A critical parameter determining the strength of the bond between the protective coating and the substrate is adhesion. Low adhesion can lead to partial or complete destruction of the coating, ultimately compromising its protective properties. The results from the scratch test show that the coating undergoes destruction in two distinct stages. In the first stage, the coating cracks at force values ranging from 2.5 to 4.5 F_{zN}. As the force increases, in the second stage (from 2.6 to 7 N), the coating begins to delaminate from the substrate alloy. This two-stage destruction process is confirmed by the microscopic images of the scratches obtained after the adhesion test, which clearly depict the stages of coating failure. The adhesion of the coatings we obtained ranged within the range of 4.5 N. This value is relatively modest compared to other coatings. For instance, Yifei Zhang [11] conducted studies using pure TiN and TaN coatings, which were deposited on metallic dental implants. The scratch test results revealed that the adhesion force for TaN was approximately 26.7 N, while the adhesion force for the pure TiN coating was around 12.1 N. Considering the demanding operating conditions of prosthetic elements, it seems that the adhesion strength should ideally be higher. Although many researchers have demonstrated promising properties for coatings, there is an ongoing search for better solutions to achieve

permanent and strong adhesion [39]. It is evident that stronger adhesion would improve the overall performance of the coating.

Thickness measurements of the obtained coatings indicate that their thickness falls within the range of 2 to 2.5 µm. This thickness should be sufficient to provide effective protective properties against corrosion and the release of potentially harmful ions from the substrate alloy. Similar thicknesses in Ti(C,N)-type coatings have been shown to offer adequate protection against corrosion [16]. However, for full confirmation of the coatings' protective capabilities, further testing focused on corrosion resistance and ion release is necessary. Microscopic examinations of the coatings revealed that they are well-sealed and free from any visible defects, such as discontinuities or porosity, which could compromise their protective properties. Pettersson et al. [37] obtained Si(C,N) coatings with a thickness ranging from 0.4 to 0.9 µm, with them exhibiting the lowest wear values. The authors suggest that when applied to a cobalt–chromium alloy substrate, such coatings may be more prone to damage. It is also important to consider that the coating thickness may influence both adhesion strength and its durability, as well as its wear resistance during the use of prosthetic elements [38]. Table 6 presents a comparison of selected mechanical properties between Si(C, N) and Ti(C, N) coatings.

Table 6. Table show the mechanical properties of the proposed Si(C,N) coating and Ti(C,N).

Type of Coating	Si(C,N)	Ti(C,N)
Hardness	15 GPa	20 GPa
Moduli of elasticity	170 GPa	270 GPa
Adhesion strength	4.5 N	12.1 N
Coatings thickness	2 to 2.5 µm	2–4 µm
Application	Fixed and removable dentures Orthodontic arches and brackets	Fixed and removable dentures Orthodontic arches and brackets

It can be concluded that, from the perspective of applying Si(C,N) coatings in prosthetics and orthodontics, the obtained results regarding mechanical properties and coating structure are fully satisfactory. These coatings are expected to offer adequate durability during the use of prosthetic and orthodontic elements, provided that their adhesion to the substrate is further enhanced.

Further research should focus on improving the adhesion of coatings to the metal substrate. Key areas of investigation should include optimizing substrate preparation techniques prior to coating application. Additionally, considering that prosthetic elements such as bridges and crowns are typically veneered with ceramics, it is crucial to examine how Si(C,N) coatings influence the adhesion between the veneering ceramics and the metal substructure.

5. Conclusions

1. The properties of the produced Si(C,N) coatings are adequate for their intended use as protective coatings for prosthetic and orthodontic elements.
2. The adhesion of the produced coatings to the Ni-Cr alloy substrate is insufficient.
3. It is necessary to continue further research to assess the biocompatibility and antibacterial properties of silicon nitride coatings on the surface of nickel–chromium alloys used in prosthetics. Assessment of the corrosion degradation and tribology of these coatings is also important.

Author Contributions: Conceptualization, Z.K. and L.K.; methodology, Z.K., L.K. and K.D.; validation, Z.K. and L.K.; formal analysis, L.K., Z.K. and K.D.; investigation, Z.K. and L.K.; resources, Z.K.; data curation, Z.K.; writing—original draft preparation, Z.K. and L.K.; writing—review and editing,

K.D.; visualization, L.K.; supervision, L.K.; project administration, Z.K. All authors have read and agreed to the published version of the manuscript.

Funding: This research received no external funding.

Data Availability Statement: Data are contained within the article.

Conflicts of Interest: The authors declare that there are no conflicts of interest regarding the publication of this paper.

References

1. Slokar, L.; Pranjić, J.; Carek, A. Metallic materials for use in dentistry. *Holist. Approach Environ.* **2017**, *7*, 39–58.
2. Reclaru, L. Corrosion behaviour of cobalt–chromium dental alloys doped with precious metals. *Biomaterials* **2005**, *26*, 4358–4365.
3. Ming, P. Corrosion behavior and cytocompatibility of a Co–Cr and two Ni–Cr dental alloys before and after the pretreatment with a biological saline solution. *RSC Adv.* **2017**, *7*, 5843–5852.
4. Ercetin, A.; Özgün, Ö.; Aslantaş, K.; Der, O.; Yalçın, B.; Şimşir, E.; Aamir, M. Microstructural and Mechanical Behavior Investigations of Nb-Reinforced Mg–Sn–Al–Zn–Mn Matrix Magnesium Composites. *Metals* **2023**, *13*, 1097. [CrossRef]
5. Hou, C.-H.; Ye, Z.-S.; Qi, F.-G.; Wang, Q.; Li, L.-H.; Ouyang, X.-P.; Zhao, N. Effect of Al addition on microstructure and mechanical properties of Mg−Zn−Sn−Mn alloy. *Trans. Nonferrous Met. Soc. China* **2021**, *31*, 1951–1968. [CrossRef]
6. Szymanowski, H.; Sobczyk, A.; Gazicki-Lipman, M.; Jakubowski, W.; Klimek, L. Plasma enhanced CVD deposition of titanium oxide for biomedical applications. *Surf. Coat. Technol.* **2005**, *200*, 1036–1040.
7. Kula, Z.; Semenov, M.; Klimek, L. Carbon Coatings Deposited on Prosthodontic Ni-Cr Alloy. *Appl. Sci.* **2021**, *11*, 4551. [CrossRef]
8. Chouirfa, H.; Bouloussa, H.; Migonney, V.; Falentin-Daudré, C. Review of titanium surface modification techniques and coatings for antibacterial applications. *Acta Biomater.* **2019**, *83*, 37–54.
9. Dong, H.; Liu, H.; Zhou, N.; Li, Q.; Yang, G.; Chen, L.; Mou, Y. Surface modified techniques and emerging functional coating of dental implants. *Coatings* **2020**, *10*, 1012. [CrossRef]
10. Kaloyeros, A.E.; Jove, F.; Goff, J.; Arkles, B. Review—Silicon Nitride and Silicon Nitride-Rich Thin Film Technologies: Trends in Deposition Techniques and Related Applications. *ECS J. Solid State Sci. Technol.* **2017**, *6*, 691–714.
11. Zhang, Y.; Zheng, Y.; Li, Y.; Wang, L.; Bai, Y.; Zhao, Q.; Xiong, X.; Cheng, Y.; Tang, Z.; Deng, Y.; et al. Tantalum Nitride-Decorated Titanium with Enhanced Resistance to Microbiologically Induced Corrosion and Mechanical Property for Dental Application. *PLoS ONE* **2015**, *10*, e0130774. [CrossRef]
12. Narayan, R. Nanostructured diamond like carbon thin films for medical applications. *Mater. Sci. Eng. C* **2005**, *25*, 405–416.
13. Banaszek, K.; Maślanka, M.; Semenov, M.; Klimek, L. Corrosive Studies of a Prosthetic Ni-Cr Alloy Coated with Ti(C,N) Type Layers. *Materials* **2022**, *15*, 2471. [CrossRef] [PubMed]
14. Jamesh, M.I.; Li, P.; Bilek, M.M.; Boxman, R.L.; McKenzie, D.R.; Chu, P.K. Evaluation of corrosion resistance and cytocompatibility of graded metal carbon film on Ti and NiTi prepared by hybrid cathodic arc/glow discharge plasma-assisted chemical vapor deposition. *Corros. Sci.* **2015**, *97*, 126–138.
15. Hsu, S.-M.; Fares, C.; Xia, X.; Rasel, M.A.J.; Ketter, J.; Afonso Camargo, S.E.; Haque, M.A.; Ren, F.; Esquivel-Upshaw, J.F. In Vitro Corrosion of SiC-Coated Anodized Ti Nano-Tubular Surfaces. *J. Funct. Biomater.* **2021**, *12*, 52. [CrossRef]
16. Banaszek, K.; Klimek, L. Ti (C, N) as Barrier Coatings. *Coatings* **2019**, *9*, 432. [CrossRef]
17. Banaszek, K.; Klimek, L.; Dąbrowski, J.R.; Jastrzębski, W. Fretting Wear in Orthodontic and Prosthetic Alloys with Ti(C, N) Coatings. *Processes* **2019**, *7*, 874. [CrossRef]
18. Liang, Y.; Liu, D.; Bai, W.; Tu, J. Investigation of silicon carbon nitride nanocomposite films as a wear resistant layer in vitro and in vivo for joint replacement applications. *Colloids Surf. B Biointerfaces* **2017**, *153*, 41–51. [PubMed]
19. Banaszek, K.; Szymanski, W.; Pietrzyk, B.; Klimek, L. Adhesion of E. coli Bacteria Cells to Prosthodontic Alloys Surfaces Modified by TiO2 Sol-Gel Coatings. *Adv. Mater. Sci. Eng.* **2013**, *2013*, 179241.
20. Knowles, B.R. Zwitterion functionalized silica nanoparticle coatings: The effect of particle size on protein, bacteria, and fungal spore adhesion. *Langmuir* **2018**, *35*, 1335–1345. [PubMed]
21. Akhavan, B. Plasma activated coatings with dual action against fungi and bacteria. *Appl. Mater. Today* **2018**, *12*, 72–84. [CrossRef]
22. Bazaka, K. Plasma-assisted surface modification of organic biopolymers to prevent bacterial attachment. *Acta Biomater.* **2011**, *7*, 2015–2028. [CrossRef] [PubMed]
23. Jedrzejowski, P.; Cizek, J.; Amassian, A.; Klemberg-Sapieha, J.E.; Vlcek, J.; Martinu, L. Mechanical and optical properties of hard SiCN coatings prepared by PECVD. *Thin Solid Film.* **2004**, *447*, 201–207. [CrossRef]
24. Kumar, D.; Das, S.; Swain, B.P.; Guha, S. Unveiling the multifaceted impact of C2H2 flow on SiCN CVD coatings: Mechanical mastery and beyond. *Ceram. Int.* **2024**, *50*, 6526–6542. [CrossRef]

25. Kaloyeros, A.E.; Pan, Y.; Goff, J.; Arkles, B. Silicon nitride and silicon nitride-rich thin film technologies: State-of-the-art processing technologies, properties, and applications. *ECS J. Solid State Sci. Technol.* **2020**, *9*, 063006. [CrossRef]
26. Xia, X.; Chiang, C.-C.; Gopalakrishnan, S.K.; Kulkarni, A.V.; Ren, F.; Ziegler, K.J.; Esquivel-Upshaw, J.F. Properties of SiCN Films Relevant to Dental Implant Applications. *Materials* **2023**, *16*, 5318. [CrossRef]
27. Xie, E.; Ma, Z.; Lin, H.; Zhang, Z.; He, D. Preparation and characterization of SiCN films. *Opt. Mater.* **2003**, *23*, 151–156. [CrossRef]
28. Fares, C.; Hsu, S.; Xian, M.; Xia, X.; Ren, F.; John, J.; Mecholsky, J.J., Jr.; Gonzaga, L.; Esquivel-Upshaw, J. Demonstration of a SiC Protective Coating for Titanium Implants. *Materials* **2020**, *13*, 3321. [CrossRef] [PubMed]
29. Skjöldebrand, C.; Hulsart-Billström, G.; Engqvist, H.; Persson, C. Si–Fe–C–N Coatings for Biomedical Applications: A Combinatorial Approach. *Materials* **2020**, *13*, 2074. [CrossRef] [PubMed]
30. Afonso Camargo, S.E.; Mohiuddeen, A.S.; Fares, C.; Partain, J.L.; Carey, P.H., IV; Ren, F.; Hsu, S.-M.; Clark, A.E.; Esquivel-Upshaw, J.F. Anti-Bacterial Properties and Biocompatibility of Novel SiC Coating for Dental Ceramic. *J. Funct. Biomater.* **2020**, *11*, 33. [CrossRef] [PubMed]
31. Walczak, M.; Drozd, K. Tribological characteristics of dental metal biomaterials. *Curr. Issues Pharm. Med. Sci.* **2016**, *29*, 158–162. [CrossRef]
32. Nine, M.J.; Choudhury, D.; Hee, A.C.; Mootanah, R.; Osman, N.A. A: Wear Debris Characterization and Corresponding Biological Response. Artificial Hip and Knee Joints. *Materials* **2014**, *7*, 980. [CrossRef] [PubMed]
33. Xu, L.-J.; Xiao, S.-L.; Jing, T.; Chen, Y.-Y.; Huang, Y.-D. Microstructure and dry wear properties of Ti-Nb alloys for dental prostheses. *Trans. Nonferrous Met. Soc. China* **2009**, *19*, 639. [CrossRef]
34. Milojević, S.; Savić, S.; Mitrović, S.; Marić, D.; Krstić, B.; Stojanović, B.; Popović, V. Solving the Problem of Friction and Wear in Auxiliary Devices of Internal Combustion Engines on the Example of Reciprocating Air Compressor for Vehicles. *Tehnicki vjesnik-Tech. Gazette* **2023**, *30*, 122–130. [CrossRef]
35. Klimek, L.; Makówka, M.; Sobczyk-Guzenda, A.; Kula, Z. Characteristics of Si (C,N) Silicon Carbonitride Layers on the Surface of Ni–Cr Alloys Used in Dental Prosthetics. *Materials* **2024**, *17*, 2450. [CrossRef]
36. Chiang, C.-C.; Xia, X.; Craciun, V.; Rocha, M.G.; Camargo, S.E.A.; Rocha, F.R.G.; Gopalakrishnan, S.K.; Ziegler, K.J.; Ren, F.; Esquivel-Upshaw, J.F. Enhancing the Hydrophobicity and Antibacterial Properties of SiCN-Coated Surfaces with Quaternization to Address Peri-Implantitis. *Materials* **2023**, *16*, 5751. [CrossRef] [PubMed]
37. Pettersson, M.; Berlind, T.; Schmidt, S.; Jacobson, S.; Hultman, L.; Persson, C.; Engqvist, H. Structure and composition of silicon nitride and silicon carbon nitride coatings for joint replacements. *Surf. Coat. Technol.* **2013**, *235*, 827–834. [CrossRef]
38. Grigoriev, S.; Sotova, C.; Vereschaka, A.; Uglov, V.; Cherenda, N. Modifying Coatings for Medical Implants Made of Titanium Alloys. *Metals* **2023**, *13*, 718. [CrossRef]
39. Li, X.; Bhushan, B. A review of nanoindentation continuous stiffness and its applications. *Mater. Charact.* **2002**, *48*, 11–36. [CrossRef]
40. Anthony, C. Fisher-Cripps. In *Nanoindentation*, 2nd ed.; Winer, W.O., Bergles, A.E., Eds.; Mechanical Engineering Series; Springer: Killarney Heights, Australia, 2004.

Disclaimer/Publisher's Note: The statements, opinions and data contained in all publications are solely those of the individual author(s) and contributor(s) and not of MDPI and/or the editor(s). MDPI and/or the editor(s) disclaim responsibility for any injury to people or property resulting from any ideas, methods, instructions or products referred to in the content.